Published Ahead of Print on October 3, 2022 as 10.1212/WNL.0000000000201465

OPEN

Neurology®
The most widely read and highly cited peer-reviewed neurology journal
The Official Journal of the American Academy of Neurology

AMERICAN ACADEMY OF NEUROLOGY®

Neurology Publish Ahead of Print
DOI: 10.1212/WNL.0000000000201465

Differentiating Multiple Sclerosis From AQP4-Neuromyelitis Optica Spectrum Disorder and MOG-Antibody Disease With Imaging

Author(s):
Rosa Cortese, PhD[1, 2]; Ferran Prados Carrasco, PhD[1,3,4]; Carmen Tur, MD, PhD[1,5]; Alessia Bianchi, MD[1]; Wallace Brownlee, MD[1]; Floriana De Angelis, MD, PhD[1]; Isabel De La Paz, MSc[1]; Francesco Grussu, PhD[1,6]; Lukas Haider, PhD[1,7]; Anu Jacob, PhD[8,9]; Baris Kanber, PhD[3]; Lise Magnollay, PhD[1]; Richard S Nicholas, PhD[10]; Anand Trip, PhD[1,11]; Marios Yiannakas, PhD[1]; Ahmed T. Toosy, FRCP[1]; Yael Hacohen, PhD, MRCPCH[1]; Frederik Barkhof, MD, PhD[1,3,11,12]; Olga Ciccarelli[1,11]

Corresponding Author:
Olga Ciccarelli, o.ciccarelli@ucl.ac.uk

Affiliation Information for All Authors: 1. Queen Square MS Centre, Department of Neuroinflammation, UCL Queen Square Institute of Neurology, Faculty of Brain Science, University College of London; 2. Department of Medicine, Surgery and Neuroscience, University of Siena, Siena, Italy; 3. Centre for Medical Imaging Computing, Department of Medical Physics and Biomedical Engineering, University College of London, London; 4. Universitat Oberta de Catalunya, Barcelona, Spain; 5. MS Centre of Catalonia (Cemcat), Vall d'Hebron Institute of Research, Vall d'Hebron Barcelona Hospital Campus, Spain; 6. Radiomics Group, Vall d'Hebron Institute of Oncology, Vall d'Hebron Barcelona Hospital Campus, Barcelona, Spain; 7. Department of Biomedical Imaging and Image Guided Therapy, Medical University of Vienna, Währingergürtel 18-20 A-1090 Vienna, Austria; 8. NMO Clinical Service at the Walton Centre, Liverpool, United Kingdom; 9. Division Of Multiple Sclerosis and Autoimmune Neurology, Neurological Institute, Cleveland Clinic Abu Dhabi, United Arab Emirates; 10. Division of Brain Sciences, Department of Medicine, Imperial College London; 11. National Institute for Health Research (NIHR) University College London Hospitals (UCLH) Biomedical Research Centre, London; 12. Department of Radiology and Nuclear Medicine, Amsterdam University Medical Centre, the Netherlands

Equal Author Contribution:

Contributions:
Rosa Cortese: Drafting/revision of the manuscript for content, including medical writing for content; Major role in the acquisition of data; Study concept or design; Analysis or interpretation of data
Ferran Prados Carrasco: Analysis or interpretation of data
Carmen Tur: Analysis or interpretation of data
Alessia Bianchi: Major role in the acquisition of data
Wallace Brownlee: Major role in the acquisition of data
Floriana De Angelis: Major role in the acquisition of data; Analysis or interpretation of data
Isabel De La Paz: Analysis or interpretation of data
Francesco Grussu: Analysis or interpretation of data
Lukas Haider: Analysis or interpretation of data
Anu Jacob: Major role in the acquisition of data
Baris Kanber: Analysis or interpretation of data
Lise Magnollay: Major role in the acquisition of data
Richard S Nicholas: Major role in the acquisition of data
Anand Trip: Major role in the acquisition of data
Marios Yiannakas: Major role in the acquisition of data
Ahmed T. Toosy: Major role in the acquisition of data; Analysis or interpretation of data
Yael Hacohen: Major role in the acquisition of data; Analysis or interpretation of data
Frederik Barkhof: Analysis or interpretation of data
Olga Ciccarelli: Drafting/revision of the manuscript for content, including medical writing for content; Study concept or design; Analysis or interpretation of data

Figure Count:
3

Table Count:
4

Search Terms:
[40] All Demyelinating disease (CNS), [41] Multiple sclerosis, [42] Devic's syndrome, [120] MRI, [322] Class II

Acknowledgment:

Study Funding:
The authors report no targeted funding

Disclosures:
R. Cortese was awarded a MAGNIMS-ECTRIMS fellowship in 2019. F. Prados is a non-clinical Guarantors of the Brain fellow. C. Tur is currently being funded by a Junior Leader La Caixa Fellowship. The project that gave rise to these results received the support of a fellowship from "la Caixa" Foundation (ID 100010434). The fellowship code is LCF/BQ/PI20/11760008. She has also received the 2021 Merck's Award for the Investigation in MS, awarded by the Merck Foundation. In 2015, she received an ECTRIMS Post-doctoral Research Fellowship and has received funding from the UK MS Society. She has also received honoraria from Roche and Novartis. A. Bianchi has nothing to disclose. W. Brownlee has participated in advisory boards and/or received speaker honoraria for Biogen, Celgene, Merck Serono, Mylan, Novartis, Sanofi and Roche. F. De Angelis has nothing to disclose. I. De La Paz has nothing to disclose. F. Grussu is currently supported by PREdICT, a study at the Vall d'Hebron Institute of Oncology in Barcelona funded by AstraZeneca. L. Haider was awarded a MAGNIMS-ECTRIMS fellowship in 2019. A. Jacob has nothing to disclose. B. Kanber is supported by the National Institute for Health Research Biomedical Research Centre at University College London Hospitals NHS Foundation Trust and University College London. L. Magnollay has nothing to disclose. R. Nicholas has carried out advisory boards for Biogen, Roche and Novartis. He is supported by the NIHR Biomedical Research Centre initiative at Imperial College. He has received research funding from UK and National MS societies and PDUK. A. Trip is supported by the NIHR Biomedical Research Centre initiative at UCLH and received honoraria from Biogen, Merck Serono, Novartis, Roche and Teva for educational activities and advisory boards. M. Yiannakas has nothing to disclose. Ahmed T. Toosy has received speaker honoraria from Biomedia, Sereno Symposia International Foundation, Bayer and meeting expenses from Biogen Idec and Novartis He was the UK PI for two clinical trials sponsored by MEDDAY. Yael Hacohen has nothing to disclose. F. Barkhof is supported by the NIHR Biomedical Research Centre initiative at UCLH, and he serves on the editorial boards of Brain, European Radiology, Journal of Neurology, Neurosurgery & Psychiatry, Neurology, Multiple Sclerosis, and Neuroradiology, and serves as consultant for Bayer Schering Pharma, Sanofi-Aventis, Biogen-Idec, TEVA Pharmaceuticals, Genzyme, Merck-Serono, Novartis, Roche, Synthon, Jansen Research, and Lundbeck. O. Ciccarelli received research funding from NIHR Biomedical Research Centre initiative at UCLH, UK and National MS Societies, Rosetrees trust; she is an Associate Editor for Neurology. She acts as a consultant for Novartis and Merck.

Preprint DOI:

Received Date:
2022-01-18

Accepted Date:
2022-09-09

Handling Editor Statement:
Submitted and externally peer reviewed. The handling editor was Elizabeth Silbermann, MD.

Abstract:

Background and objectives: Relapsing remitting multiple sclerosis (RRMS), aquaporin4 antibody-positive neuromyelitis optica spectrum disorder (AQP4-NMOSD) and myelin oligodendrocyte glycoprotein antibody-associated disease (MOGAD) may have overlapping clinical features. There is an unmet need for imaging markers that differentiate between them when serologic testing is unavailable or ambiguous. We assessed whether imaging

characteristics typical of MS discriminate RRMS from AQP4-NMOSD and MOGAD, alone and in combination.

Methods: Adult, non-acute patients with RRMS, APQ4-NMOSD, MOGAD and healthy controls, were prospectively recruited at the National Hospital for Neurology and Neurosurgery (London, UK), and the Walton Centre (Liverpool, UK) between 2014 and 2019. They underwent conventional and advanced brain, cord and optic nerve MRI, and optical coherence tomography.

Results: A total of 91 consecutive patients (31 RRMS, 30 APQ4-NMOSD, 30 MOGAD) and 34 healthy controls were recruited. The most accurate measures differentiating RRMS from AQP4-NMOSD were the proportion of lesions with the central vein sign (CVS) (84% vs. 33%, accuracy/specificity/sensitivity: 91/88/93%, p<0.001), followed by cortical lesions (median: 2 [range: 1-14] vs. 1 [0-1], accuracy/specificity/sensitivity: 84/90/77%, p=0.002), and white matter lesions (mean: 39.07 [±25.8] vs. 9.5 [±14], accuracy/specificity/sensitivity: 78/84/73%, p=0.001). The combination of higher proportion of CVS, cortical lesions and optic nerve magnetization transfer ratio reached the highest accuracy in distinguishing RRMS from AQP4-NMOSD (accuracy/specificity/sensitivity: 95/92/97%, p<0.001).

The most accurate measures favouring RRMS over MOGAD were: white matter lesions (39.07 [±25.8] vs. 1 [±2.3], accuracy/specificity/sensitivity: 94/94/93%, p=0.006), followed by cortical lesions (2 [1-14] vs. 1 [0-1], accuracy/specificity/sensitivity: 84/97/71%, p=0.004), and retinal nerve fibre layer thickness (RNFL) (mean: 87.54 [±13.83] vs 75.54 [±20.33], accuracy/specificity/sensitivity: 80/79/81%, p=0.009). Higher cortical lesion number combined with higher RNFL thickness best differentiated RRMS from MOGAD (accuracy/specificity/sensitivity: 84/92/77%, p<0.001).

Discussion: Cortical lesions, CVS and optic nerve markers achieve a high accuracy in distinguishing RRMS from APQ4-NMOSD and MOGAD. This information may be useful in

clinical practice, especially outside the acute phase and when serologic testing is ambiguous or not promptly available.

Classification of Evidence: This study provides Class II evidence that selected conventional and advanced brain, cord, and optic nerve MRI and OCT markers distinguish adult patients with RRMS from APQ4-NMOSD and MOGAD.

Manuscript

Introduction

Multiple sclerosis (MS) has a wide range of clinical and imaging manifestations, which overlap with those of neuromyelitis optica spectrum disorders (NMOSD) and myelin oligodendrocyte glycoprotein antibody-associated disease (MOGAD).[1] Serological testing of Aquaporin4 (AQP4) antibody (Ab) and MOG-Ab with cell-based assays (CBA) have high specificity.[2,3] However, these assays are not widely available and may have variable sensitivity[4], leading to false-negative results[5]. When patients are tested indiscriminately, false-positive MOG-Ab results are seen in 28% of cases.[6] In addition, antibody levels may fluctuate, and outside an acute event they may be negative in up to 57% of MOGAD patients[7] and decline up to become negative in the remission phase of NMOSD.[8,9] When serologic testing is unavailable or ambiguous, or a false negative serological result is suspected, MRI can be of value to support the differential diagnosis.

Differences in patterns of brain and spinal cord lesions between RRMS, AQP4-NMOSD and MOGAD have been described.[10,11] In RRMS white matter lesions tend to affect specific brain regions, such as the periventricular and juxta-cortical white matter, the corpus callosum, and

the infratentorial areas[12], while in AQP4-NMOSD brain abnormalities are frequently located in areas with high AQP4 expression (e.g. peri-ependymal lesions surrounding the ventricles, or involving corticospinal tracts).[13] In adult MOGAD, brain MRI can be unremarkable or show large, ill-defined or defined lesions, mostly located in the deep grey matter and in the cerebellar peduncles.[14] Longitudinally extensive transverse myelitis (LETM) is the hallmark of AQP4-NMOSD with predilection for the cervical cord, while in MS multiple, short segment lesions are common, mostly located in the cervical cord. In MOGAD, cord lesions often affect the lower thoracic cord and conus, and tend to be longitudinally extensive in the acute stage.[15] Imaging features which are very suggestive of a specific disease, may not be seen any more in the non-acute phase; this is common in patients with MOGAD.[16] In addition, the approach of reaching a diagnosis of one of these three diseases on the basis of typical MRI features alone (or in combination) is not standardized.[17]

With regard to advanced MRI markers, cortical lesions are well described as distinctive features of MS,[18] while they are rarely seen in AQP4-NMOSD and MOGAD.[19,20] The CVS is detectable in a higher percentage of brain lesions in RRMS than AQP4-NMOSD[21] and MOGAD.[22] Grey matter atrophy is seen in MS, but not in NMOSD;[23] it is unknown whether grey matter volumes distinguish between RRMS and MOGAD. Previous studies showed a greater cervical cord atrophy in AQP4-NMOSD than in RRMS, but no cord atrophy was detected in MOGAD.[24,25] While microstructural damage of the cord in RRMS and AQP4-NMOSD was found using diffusion tensor imaging (DTI), no substantial changes were detected in MOGAD.[25]

Optic neuritis is a common feature of these three diseases. In RRMS, optic nerve lesions on orbital MRI are often unilateral, short and anterior, while in AQP4-NMOSD and MOGAD

they are mostly bilateral and long, although posterior in the former and anterior in the latter.[26] Optic nerve atrophy and microstructural damage can be detected with quantitative MRI techniques.[27] There have been no previous studies using magnetization transfer ratio (MTR) of the optic nerve in the different segments of NMOSD patients, while studies in MS showed no definitive results.[28,29] Optical coherence tomography (OCT)[30] has been widely used in MS, demonstrating a thinner retinal nerve fibre layer (RNFL) in AQP4-NMOSD than MS,[31] while showing conflicting results when comparing the three diseases.[32] It is unknown whether the inclusion of optic nerve markers might improve the differentiation between MS and the two antibody-mediated diseases in the non-acute phase.

The primary research question of this study is to identify selected conventional and advanced brain, cord, and optic nerve MRI and OCT markers to distinguish adult patients with RRMS from APQ4-NMOSD and MOGAD. We investigated whether MRI characteristics, known to be typical of MS, discriminate between RRMS and the two antibody-mediated diseases alone and in combination, and whether including optic nerve imaging measures may enhance the accuracy of the discrimination.

Methods

Subjects

Patients over the age of 18 years with a diagnosis of (1) RRMS according to 2017 McDonald criteria[1] (2) AQP4-NMOSD according to Wingerchuk criteria[33] or (3) MOGAD (defined as MOG-Ab positivity using CBA in the context of an acute demyelinating event in patients presenting with a MOGAD phenotype previously described[34]), seen at the National Hospital for Neurology and Neurosurgery, London, and the NMO Clinical Service at the Walton

Centre, Liverpool, between 2014-2019, were recruited consecutively. Antibody testing using either live or fixed CBA was performed as part of the clinical evaluation in the local, clinical laboratories. The threshold for serum MOG-Ab CBA positivity was IgG1 at 1:20, followed by 1:200 for H&L secondary antibody. To avoid the inclusion of false positives, only patients with a 'secure' positivity without low or borderline autoantibodies results, were included. Age- and sex-matched healthy controls were also recruited. Participants were excluded if they had major contraindications to MRI, a neurological comorbidity, any ophthalmic conditions (such as glaucoma, ocular trauma, or degenerative eye disease), or a relapse in the previous 6 months. Data from a subgroup of these patients have been previously reported.[21]

Clinical assessment and OCT

At the time of the MRI, patients' disability was assessed using the Expanded Disability Status Scale (EDSS), the timed 25-foot walk test (TWT), the 9-hole peg test (9-HPT) and the Symbol Digit Modalities Test (SDMT)[35]. Visual assessments for each eye were performed using high contrast letter acuity (VA100%) with a retro-illuminated Early Treatment Diabetic Retinopathy Study chart at 4 metres, and low contrast letter acuity (LCLA) with a retro-illuminated 2.5%, and 1.25% Sloan charts.

Patients and controls underwent peripapillary RNFL and macular volume OCT scanning using Heidelberg Eye Explore 1.10.2.0 (Spectralis-version 6.9a, Heidelberg Engineering, Germany). Peripapillary RNFL and macular GCIPL thickness were extracted. A quality check was performed according to international OSCAR-IB criteria.[36]

MRI data acquisition and analysis

All participants underwent a 3T MRI scan at the Queen Square MS Centre, London, using a 32-channel head coil (see protocol details in **eTable 1).**

Brain T2-lesions were semi-automatically segmented using JIM v.6.0, whilst cervical cord lesions were manually identified on sagittal T2-weighted and axial FFE scans.

For brain tissue parcellation, we used the geodesic information flows (GIF) method,[37] after an automated T1 brain lesion-filling technique.[38] The fractional volumes of white matter, grey matter, and deep grey matter relative to total intracranial volume (i.e, WMF, GMF and deep GMF) were calculated.

Cortical lesions were manually identified on PSIR images and scored as leukocortical or intracortical[39] by consensus between two raters (R.C. and L.H.) and a senior neuroradiologist (F.B.), who reviewed the cases of disagreement.

For the CVS analysis, the T2-weighted images were affine co-registered to the SWI using a symmetric and inverse-consistent approach. The identification of the CVS (indicating the presence of a central vessel, predominantly veins and venules, in MS plaques) was obtained on SWI with the fully blinded analysis previously described[21] and following the NAIMS criteria[40]. The proportion of lesions with the CVS out of the total number of lesions was reported. The presence of the CVS was based on the consensus between two raters (R.C. and L.H.).

The mean cross-sectional area (CSA) of the cord was calculated at C2-C3, using the active surface model (JIM v.6.0).[41]

Diffusion weighted images (DWI) were processed using FSL and the SCT (FMRIB Software Library v.0.5).[42,43] The mean values of diffusion metrics within the whole cord were calculated (see **eFigure 1**).

MTI acquisition was performed separately for each eye; the mean MTR values in the intra-orbital, intra-canicular and intra-cranial optic nerve were obtained (see **eFigure 2**).

Raters worked independently, blinded to clinical data; they had a good inter-rater agreement (Cohen kappa coefficients $\geq$ 92%).

During the study, a major MRI system upgrade took place (new scanner software, from release 3 to 5; new hardware, from Philips Achieva to Ingenia-CX), which was considered in the statistical analysis.

Statistical analysis

Age, sex, clinical and lesion characteristics were compared between RRMS, AQP4-NMOSD, MOGAD and healthy control groups using $\chi 2$ test, linear regression, Mann-Whitney U tests or mixed effect regression models, depending on the nature of the variable.

The analyses for this study were then divided into the following 2 parts:

1. **Differences in brain, cervical cord and optic nerve measures between diseases and their association with clinical measures**

Multiple linear regression models were fitted to evaluate differences in brain and cord MRI metrics between groups and their associations with clinical measures. The following analyses were performed: (i) estimation of differences in brain and cord MRI measures (lesions, BPF, GMF, deep GMF, WMF, CSA, DTI metrics) between the three patient groups and controls, where MRI measures were the dependent variables and "patient group" the explanatory variable; (ii) assessment of correlations between MRI metrics, and clinical measures in each patient group separately, where clinical measures were the dependent variables (one at a time) and MRI metrics the explanatory variables.

Random intercept mixed-effects regression models were used to assess differences between patient groups in optic nerve metrics (visual acuity, average RNFL and GCIPL thickness, and average MTR of the whole optic nerve and each segment) between patient groups and

between patients and controls, with a group indicator as the main covariate. Multiple mixed-effect regressions were used to assess correlations between optic nerve metrics different between patients and controls and clinical measures in each group. These models enabled us to perform the analyses considering that the observations corresponding to each pair of eyes were correlated and belonged to the same subject.

2. Identifying imaging markers which discriminate between diseases

To identify the MRI and OCT variables discriminating between diseases, the variables which showed significant differences between any disease group pair were entered into forward stepwise logistic regression models. First, we ran univariable logistic regression analyses, with "patient group" as the dependent variable, and "MRI measures" as covariates, one at a time. For optic nerve measures, the average between the two eyes was used. To select the best set of predictors, each imaging measure was added individually to a model already adjusted for age, sex and upgrade. If these imaging measures one at a time were significant, were kept for the next stage, added sequentially to the basic model and kept if significant. The order of this addition was determined by the individual accuracy of the measures. If two variables had individually the same accuracy, then the variable with the lowest BIC was chosen first. From all models, we obtained the odds ratio (OR) of having one disease vs another (i.e., RRMS vs AQP4-NMOSD, RRMS vs MOGAD, AQP4-NMOSD vs MOGAD), the accuracy, and the area under the curve (AUC) ROC (Receiving Operated Characteristic curve).

In each group, for each imaging predictor, the best cut-off (i.e., the value associated with the highest accuracy) that predicted the outcome (e.g., a diagnosis of RRMS vs AQP4-NMOSD or MOGAD) was calculated.

All the analyses were corrected for age, sex and upgrade of the scanner. Other potential confounders, such as disease duration, presence of brain or cervical cord lesions and atrophy measures in the brain and the spinal cord, number of optic neuritis were also considered, as appropriate.

Analyses were performed in Stata 15.1 software (Stata Corporation, College Station, Texas, USA). Statistical significance was considered when p-values were <0.01.

Data Availability

Anonymized data not published within this article will be made available by request from any qualified investigator.

Standard Protocol Approvals, Registrations, and Patient Consents

Written informed consent was obtained from all participants. The study was approved by the NRES Committee London Bloomsbury and complied with the Data Protection Act 2018.

Results

Participant characteristics

A total of 91 patients (31 RRMS, 30 AQP4-NMOSD, 30 MOGAD) and 34 healthy controls were included in the study (flowchart of patients is given in **eFigure 3**). Thirty (100%) AQP4-NMOSD and 25 (83%) MOGAD patients were tested using live CBA, while the remaining using fixed assays. Patients with AQP4-NMOSD had the highest EDSS and the worst high- and low-contrast visual acuity, whilst patients with MOGAD were the youngest and had the shortest disease duration (all

p<0.001). A relapsing disease course was reported in 87% patients with AQP4-NMOSD and 67% patients with MOGAD. The most common clinical presentations at onset in the two antibody-mediated diseases were optic neuritis and transverse myelitis. **(Table 1).** Details about MOG-Ab testing timing are provided in **eTable 2.**

Differences in brain, cervical cord and optic nerve MRI, and OCT measures between the three diseases.

Differences between diseases are summarised in **Table 2**. Brain white matter lesions were detected in 100% of RRMS, 83% of AQP4-NMOSD, and 27% of MOGAD patients. The mean number and volume of lesions were higher in RRMS than AQP4-NMOSD (p<0.001) and MOGAD (p<0.001, p=0.007). No difference in brain lesion number or volume between AQP4-NMOSD and MOGAD was identified **(Figure 1)**.

The presence of at least one cervical cord lesion was more common in RRMS (55% of the cases) than AQP4-NMOSD (40%) and MOGAD (4%) (p<0.001).

Patients with RRMS showed lower brain parenchymal fraction, white matter fraction and deep grey matter fraction than healthy controls (p<0.001, p=0.009 and p<0.001, respectively), lower brain parenchymal fraction and deep grey matter fraction than AQP4-NMOSD (p=0.005 and p=0.001, respectively), and lower deep grey matter fraction than MOGAD (p<0.001). Patients with MOGAD did not differ from healthy controls and from AQP4-NMOSD.

Cortical lesions were detected in 73% of MS patients, 4% of AQP4-NMOSD patients and 3% of MOGAD patients. There was a higher number of cortical lesions in RRMS (total of 74: 40 leukocortical and 34 intracortical, with a median of 2 lesions per patient) than AQP4-

NMOSD (only one leukocortical lesion in one patient) and MOGAD (only one intracortical lesion in one patient) **(Figure 2)**.

The central vein sign within white matter lesions on SWI was observed in 100% of RRMS, 70% of AQP4-NMOSD and 17% of MOGAD patients. The proportion of lesions with the CVS was higher in RRMS (84%) than AQP4-NMOSD (33%) but did not differ between AQP4-NMOSD and MOGAD **(Figure 2 and 3)**.

Both patients with RRMS and AQP4-NMOSD showed smaller cervical cord cross-sectional area than healthy controls (p=0.001 and p=0.003 respectively), whilst patients with MOGAD did not show cervical cord atrophy. Patients with AQP4-NMOSD showed lower fractional anisotropy (FA) than healthy controls (regression coefficient [RC]: -0.043, 95%CI: -0.71 to -0.014, p=0.003). No differences were found between RRMS and MOGAD and healthy controls, and between the three diseases.

All patient groups showed lower RNFL thickness than healthy controls, with the two antibody-mediated diseases also showing lower GCIPL than healthy controls (all p<0.01) **(eFigure 4)**. When compared with RRMS, GCIPL thickness was lower in AQP4-NMOSD (p=0.007), while RNFL thickness was lower in MOGAD (p=0.009). AQP4-NMOSD and MOGAD patients showed lower average MTR of the whole optic nerve and the intra-orbital segment compared to RRMS and healthy controls (all p<0.01). MOGAD showed lower MTR of the intracranial segments when compared to RRMS and healthy controls. No differences in OCT and optic nerve MTR indices were found between the two antibody-mediated diseases.

Association between clinical measures and imaging measures

In RRMS, worse 9-HPT z-score was associated with lower brain white matter fraction (RC: 0.07, 95%CI: 0.02 to 0.15, p=0.005) and lower CSA (RC: 0.04, 95%CI: 0.01 to 0.07, p=0.007), and worse high contrast VA was associated with reduced RNFL thickness (RC: -0,01, 95%CI: -0.02 to -0.004, p=0.001).

In AQP4-NMOSD, worse EDSS and TWT z-score were associated with lower cord cross-sectional area (respectively RC: -0.08, 95%CI: -0.14 to -0.03, p=0.006; RC: 0.24, 95%CI: 0.13 to 0.34, p<0.001), and worse 9-HPT and greater vibration dysfunction with lower cervical cord FA (respectively RC: 11.74, 95%CI: 6.19 to 17.28, p<0.001; RC: -72.31, 95%CI: -102.48 to -42.15, p<0.001). Worse high contrast VA was associated with lower average MTR of the whole optic nerve and the intra-orbital segment (respectively RC: -0.07, 95%CI: -0.10 to -0.03, p<0.001; RC: -0,04, 95%CI: -0.07 to -0.02, p=0.002).

In MOGAD, worse high contrast VA was associated with reduced RNFL thickness (RC: -0.004, 95%CI: -0.07 to -0.001, p=0.003), reduced GCIPL thickness (RC: -0.006, CI: -0.009 to -0.002, p=0.002), and lower average MTR of the whole optic nerve and the intra-orbital segment (respectively RC: -0.03, 95%CI: -0.05 to -0.01, p=0.001; RC: -0,03, 95%CI: -0.04 to -0.01, p<0.001).

MRI and OCT discriminators between the three diseases

RRMS vs AQP4-NMOSD

The proportion of lesions with the CVS was the most accurate measure that distinguished RRMS from AQP4-NMOSD (OR: 1.09, 95%CI: 1.05-1.14, accuracy: 91%, specificity: 88%, sensitivity: 93%, AUC: 0.93, p<0.001). This means that for each percentage unit of increase in the proportion of lesions with CVS there was a 9% increased risk of having RRMS instead

of AQP4-NMOSD. The best cut-off value that predicted RRMS was a proportion of lesions with CVS of 54%.

The second most accurate discriminator was cortical lesion number (OR: 32.52, 95%CI: 3.52-300.03, accuracy: 84%, specificity: 90%, sensitivity: 77%, AUC: 0.91, p=0.002), followed by brain white matter lesion number (OR: 1.07, 95%CI: 1.03-1.11, accuracy: 78%, specificity: 84%, sensitivity: 73%, AUC: 0.85, p=0.001), and deep GMF (OR: 0.48, 95%CI: 0.30-0.78, accuracy: 76%, specificity: 79%, sensitivity: 73%, AUC: 0.80, p=0.003). The best cut-off values that predicted RRMS were a number of cortical lesions of 1 and of brain white matter lesion of 11.

The last two significant discriminators were the brain parenchymal fraction (OR: 0.48, 95%CI: 0.28-0.83, accuracy: 66%, specificity: 72%, sensitivity: 60%, AUC: 0.76, p=0.008) and the optic nerve MTR (OR: 1.32, 95%CI: 1.04-1.68, accuracy: 66%, specificity: 60%, sensitivity: 71%, AUC: 0.73, p=0.023).

In a multivariable model, the combination of higher proportion of lesions with CVS, higher number of cortical lesions and higher average MTR of whole optic nerve achieved the highest accuracy in indicating a diagnosis of RRMS rather than AQP4-NMOSD (accuracy: 95%, specificity: 92%, sensitivity: 97%, AUC: 0.97, p<0.001) **(Table 3).**

RRMS vs MOGAD

Brain white matter lesion number was the most accurate MRI measure to predict RRMS rather than MOGAD (OR: 1.89, 95%CI: 1.20-2.99, accuracy: 94%, specificity: 94%, sensitivity: 93%, AUC: 0.99, p=0.006). This means that per each unit of increase in number

of lesions there is an 89% increase in the risk of having RRMS rather than MOGAD. The best cut-off value that predicted RRMS, was a number of white matter lesions of 5.

Other measures individually associated to a higher risk of RRMS than MOGAD were a higher number of cortical lesions (OR: 24.68, 95%CI: 2.82- 215.65, accuracy: 84%, specificity: 97%, sensitivity: 71%, AUC: 0.87, p=0.004), higher RNFL thickness (OR: 1.06, 95%CI: 1.02-1.12, accuracy: 80%, specificity: 79%, sensitivity: 81%, AUC: 0.83, p=0.009), lower deep grey matter fraction (OR: 0.24, 95%CI: 0.10-0.56, accuracy: 79%, specificity: 71%, sensitivity: 83%, AUC: 0.89, p=0.001) and higher proportion of patients with at least one cervical cord lesion (OR: 80.01, 95%CI: 4.03-1591.84, accuracy: 79%, specificity: 56%, sensitivity: 90%, AUC: 0.86, p=0.004).

The combination of higher number of cortical lesions and higher RNFL thickness achieved the highest accuracy in predicting a diagnosis of RRMS rather than MOGAD (accuracy: 84%, specificity: 92%, sensitivity: 77%, AUC: 0.94, p<0.001) **(Table 4).**

AQP4-NMOSD vs MOGAD

The presence of at least one cervical cord lesion was the only MRI measure which predicted AQP4-NMOSD than MOGAD (OR: 30.36, 95%CI: 2.15-427.88, accuracy: 71%, specificity: 65%, sensitivity: 76%, AUC: 0.68, p<0.001).

This study provides Class II evidence that selected conventional and advanced brain, cord, and optic nerve MRI and OCT markers distinguish adult patients with RRMS from APQ4-NMOSD and MOGAD.

Discussion

In this work we identified differences in brain, cervical cord and optic nerve involvement between non-acute RRMS, AQP4-NMOSD and MOGAD patient groups using different imaging modalities. The key findings are as follows: (i) the number of brain cortical and white matter lesions consistently differentiates RRMS from the two antibody-mediated diseases, while the CVS best discriminates between RRMS and AQP4-NMOSD, (ii) MTR of the optic nerve increases the accuracy in differentiating RRMS from AQP4-NMOSD, while RNFL thickness discriminates RRMS from MOGAD, (iii) AQP4-NMOSD and MOGAD share more similarities than differences, and the only imaging marker which distinguished these groups was the presence of at least one cervical cord lesion. Our findings may be particularly useful in clinical practice to support a clinical diagnosis and exclude an antibody-mediated condition when the antibody testing is unavailable or suboptimal or when there is a suspicion of false negative/positive serologic testing results.

The most accurate MRI measure that predicted RRMS rather than AQP4-NMOSD was the proportion of lesions with the central vein sign (CVS) (84% vs. 33%), extending our previous findings[21] to the wider spectrum of NMOSD. Interestingly, the CVS was detected in 78% of lesions in patients with MOGAD, which is twice as much as in AQP4-NMOSD, but it was not able to distinguish between AQP4-NMOSD and MOGAD; these findings extend the results of a previous pilot study using clinical MRI scans in a smaller number of patients.[22] A pathologic study has demonstrated that demyelinating plaques in MOGAD may arise around multiple small vessels[44], while in NMOSD demyelination is secondary to astrocytic damage, which may occlude the veins, thereby making them undetectable on MRI.[45]

The MRI marker that reached the highest accuracy in separating RRMS from MOGAD was the number of brain white matter lesions, which was also the third most accurate measure that distinguished RRMS from AQP4-NMOSD. In our study, brain MRI lesions were found in a minority of patients with MOGAD (27%), and this can be explained by two main factors. Firstly, a sizeable proportion (87%) of MOGAD patients presented with symptoms suggestive of optic neuritis and myelitis rather than ADEM or focal cortical encephalitis. Second, a complete resolution of brain lesions outside the acute phase is common in MOGAD[46], lowering the chance of finding lesions in stable patients. Therefore, our results suggest that in a patient under investigation for a suspected inflammatory demyelinating disorder, a high number of brain white matter lesions points towards a diagnosis of MS rather than MOGAD and AQP4-NMOSD. We did not look at differences in lesion distribution, due to the low number of patients with brain lesions. Further studies with larger cohorts are needed to evaluate whether different lesion location and shape may help further discriminating the diseases.

The number of cortical lesions was the second most accurate MRI marker indicating a diagnosis of RRMS rather than AQP4-NMOSD or MOGAD. While cortical demyelination is typical of MS, up to the point that the presence of cortical lesions has been introduced in the last revision of the MS diagnostic criteria,[1] they are rarely detected in NMOSD.[19] We extended these investigations to patients with MOGAD, by demonstrating that cortical lesions are not seen in non-acute patients. This is in disagreement with a neuropathological study showing subpial demyelination with cortical involvement in MOGAD, similar to that seen in MS.[44] This discrepancy may be explained by the limited ability of MRI to detect cortical lesions *in-vivo*, with the most abundant subpial demyelinating remaining unrecognized,[47] and/or by the different patient characteristics in the studies. In our cohort,

patients had adult-onset MOGAD and presented mostly with a NMOSD-like phenotype rather than ADEM, and none presented with focal cortical encephalitis.[44]

Interestingly, we demonstrated that higher MTR of the optic nerve increases the accuracy of the CVS and cortical lesions in discriminating RRMS from AQP4-NMOSD, while greater RNFL thickness achieved a high accuracy in differentiating RRMS from MOGAD, alone or in combination with cortical lesions. This is the first study assessing the discriminative role of optic nerve measures at patient level, while the majority of previous studies comparing the sensitivity of OCT and MRI measures mostly focused on the differences between eyes with and without prior optic neuritis[30], which may underestimate the effect of subclinical optic nerve involvement occurring in the three diseases.[48]

We showed that MTR may be a particularly appropriate non-conventional MRI technique to detect differences between NMOSD and RRMS, using an innovative ROI-approach as pre-processing, thus reducing the potential bias introduced by eye motion during the scans. However, this technique remains complex, and validation is crucial before developing clinical applications. Beyond non-conventional MRI, our results further support the role of OCT, which can be easily available in clinic, to objectively demonstrate a differential pattern of optic nerve involvement in the non-acute phases of the three diseases.

We found that the two antibody-mediated diseases were more similar than different in imaging characteristics and the only marker differentiating them was the presence of at least one cervical cord lesion. This is as expected and reflect the differential involvement of the spinal cord across the three diseases.[15] By contrast, no conventional cord imaging measure contributed to the differentiation between diseases, despite showing different patterns of

damage. Further studies looking at different cord segments, including sagittal and axial sequences of the thoracolumbar/conus regions are needed to accurately quantify the overall extent of cord damage in the three diseases.

Unlike cervical cord advanced MRI markers, brain atrophy contributed to discriminate between the diseases with a moderate accuracy, which is consistent with a previous study reporting the power of grey matter measures in differentiating MS from NMO using automatic classification algorithms[49] and highlight the need for an implementation of methodologies for the translation of atrophy measures in clinical practice, as they may facilitate the discrimination between MS and its mimics.[50]

Finally, whilst in RRMS and AQP4-NMOSD, brain, spinal cord and optic nerve imaging measures correlated with disability, in MOGAD we found associations only when considering optic nerve measures. This may be because the outcome measures we used may be not sufficiently sensitive in MOGAD and do not reflect patients' disabilities. More disease specific outcome measures to MOGAD, sensitive to different disabilities are needed.

This study has some limitations. First, the lack of availability of scans at disease onset did not allow us to explore the ability of imaging markers to discriminate the diseases at onset. Although we have adjusted the statistical analysis for disease duration, we studied non-acute patients, not at disease presentation. Further studies are required to evaluate if these imaging parameters are useful to distinguish patients at onset.

Secondly, some of the discriminating features are already included in the diagnostic criteria for the diseases (i.e., cortical lesions for MS, optic nerve and cervical cord involvement in NMOSD).[1,33] We have not identified distinguishing brain features between AQP-NMOSD

and MOGAD patients. Nevertheless, we did identify additional markers to differentiate MS from the two Ab-mediated diseases (CVS, atrophy, and optic nerve measures), which should be used as part of the diagnostic criteria. Future studies may investigate the added value of these imaging markers for MS diagnosis, considering also clinical and demographic variables.

Third, the cross-sectional design of the study did not allow to investigate whether the diseases differ in terms of MRI changes over time. A longitudinal analysis may identify differential patterns of inflammation and neurodegeneration that could better separate these diseases and predict the course of each demyelinating disorder.

In conclusion, a combination of cortical lesions, CVS and optic nerve markers achieves a high accuracy in distinguishing RRMS from APQ4-NMOSD and MOGAD and when especially outside the acute phase, serologic testing is unavailable or ambiguous, or a false negative serological result is suspected, these markers can be of value to support the differential diagnosis.

Tables:

Table 1: Demographic and clinical characteristics of patients with relapsing-remitting multiple sclerosis (RRMS), AQP4-neuromyelitis optica spectrum disorder (AQP4-NMOSD), myelin oligodendrocyte glycoprotein antibody disease (MOGAD) and healthy controls.

	RRMS	AQP4- NMOSD	MOGAD	Healthy controls
Number of participants	31	30	30	34
Sex (M/F)	12/19	6/24	10/20	10/24
Age at MRI, years, mean (±SD)	45.7 (±11.8)	49.4 (±12.2)	36.9 (±16.7) [a]	34.7 (±11.8)
Age at onset, years, mean (±SD)	34.9 (±9.9)	40.6 (±12.9)	31.7 (±17.9)	na
Disease duration (i.e. time from onset to MRI), years, mean (±SD)	10.9 (±6.8) [b]	8.9 (±8.1)	5.3 (±5.5)	na
EDSS, median (range)	2 (1-7.5)	4.5 (1.5-6.5) [c]	2 (1-6.5) [a]	na
TWT, z-score, mean (±SD)	-0.60 (±3.83)	-1.04 (±3.88)	0.27 (±0.61)	na
9-HPT, z-score, mean (±SD)	0.21 (±0.93)	-0.26 (±1.26)	0.02 (±0.99)	na
SDMT, mean (±SD)	51.86 (±8.64)	47.48 (±12.56)	54.41 (±16.32)	na
VA 100%, *logMAR*, mean (±SD)	0.02 (±0.28)	0.38 (±0.60) [d]	0.18 (±0.28)	na
Sloan 25, *n. letter*, mean (±SD)	16.85 (±13.17)	9.30 (±12.10) [d]	8.57 (±10.56) [e]	na
Sloan 125, *n. letter*, mean (±SD)	13.92 (±12.06)	8.71 (±11.78)	9.95 (±11.98)	na
Phenotype at onset, Number (%) patients				na
Unilateral ON	6 (19%)	16 (53%)	11 (37%)	
Bilateral ON	0	0	8 (27%)	
Isolated TM	0	6 (20%)	5 (17%)	

ON+TM	0	1 (3%)	2 (6%)	
ADEM/ADEM-like	0	0	4 (13%)	
Others	25 (81%)	7 (24%)	0	
Disease course, Number (%) patients				na
Monophasic	0	4 (13%)	10 (33%)	
Relapsing	31 (100%)	26 (87%)	20 (67%)	
CNS involvement during disease course, Number (%) patients				na
ON involvement	12 (38.7%)	20 (69.0%)	24 (80%)	
SC involvement	23 (74%)	25 (83%)	17 (57%)	
Brain involvement	31 (100%)	7 (23%)	8 (27%)	
Number of ON, mean (±SD)	0.45 (± 0.62)	1.41 (± 1.55)	2.83 (± 2.90)	na
Number of patients on treatment	30/31 (10: IFN; 8: FGY; 7: GA; 5: NAT)	27/30 (16: AZA; 6: RIT; 1: CP; 4: MMF)	15/30 (4: AZA; 11: MMF)	na

Abbreviations: 9-HPT=9-Hole Peg Test, ADEM=acute disseminated encephalomyelitis, AZA=Azathioprine, CP=Cyclophosphamide, GA=Glatiramer Acetate, IFN=Interferon, GA=Glatiramer Acetate, MMF=Mycophenolate Mofetil; LL=lower limbs, na=not available, NAT=Natalizumab, ON=optic neuritis, SD=standard deviation, SDMT=Symbol-Digit Modalities Test, RIT=Rituximab, TM=transverse myelitis, TWT=25-foot timed walk test, UL= upper limbs, VA = visual acuity.

The 9-HPT and TWT scorers were converted to z-scores, using published age-matched norms.[35]

ON involvement was defined as subacute monocular visual loss associated with pain during eye movement with objective evidence of an optic neuropathy (Toosy et al, Lancet Neurol 2014). The number of ON was calculated separately for each eye of each patient. The number reported in the table refers to the sum of events for patient.

[a] *p<0.01, obtained using linear regression to compare MOGAD to AQP4-NMOSD*

[b] *p<0.01, obtained using linear regression to compare RRMS to MOGAD*

[c] *p<0.01, obtained using linear regression to compare RRMS to AQP4-NMOSD*

[d] *p<0.01, obtained using mixed effect to compare RRMS to AQP4-NMOSD*

[e] *p<0.01, obtained using mixed effect to compare RRMS to MOGAD*

Table 2: Results obtained from brain, cervical cord, optic nerve conventional and advanced imaging metrics in RRMS, AQP4-NMOSD, MOGAD and healthy controls and comparisons between disease groups. Significant p-values (< 0.01) are in bold. The analysis was corrected for sex, age and upgrade of the scanner.

	Mean (±SD)				RRMS vs AQP4-NMOSD			RRMS vs MOGAD			AQP4-NMOSD vs MOGAD		
	RRMS	***AQP4-NMOSD***	***MOGAD***	***Healthy controls***	**RC**	**95%CI**	**p-value**	**RC**	**95%CI**	**p-value**	**RC**	**95%CI**	**p-value**
Brain*													
Number (%) of patients with brain white matter lesions	31/31 (100%)	25/30 (83%)	8/30 (27%)	5/30 (17%)	**0.184**	**0.037 to 0.331**	**0.014**[#]	**0.804**	**0.615 to 0.992**	**<0.001**[#]	**0.544**	**0.273 to 0.817**	**<0.001**[#]
Number of white matter lesions per participant, mean (±SD)[a]	39.07 (±25.82)	9.50 (±14.04)	1 (±2.30)	0.35 (±1.09)	**30.771**	**19.519 to 42.024**	**<0.001**[#]	**38.756**	**27.153 to 50.359**	**<0.001**[#]	6.05	11.70 to 23.79	0.490
Volume of brain white matter lesions, mean (±SD), mm^3 [a]	9746.29 (±9484.83)	2262.82 (±4542.15)	2524.10 (±9998.94)	272.65 (±800.00)	**7231.384**	**3471.519 to 10991.250**	**<0.001**[#]	**8620.388**	**2491.728 to 14749.050**	**0.007**[#]	1403.949	-3649.550 to 6457.448	0.580
Brain parenchymal fraction	0.745 (±0.014)	0.752 (±0.011)	0.756 (±0.019)	0.763 (±0.010)	**-0.011**	**-0.016 to 0.004**	**0.005**[#]	-0.006	-0.015 to 0.004	0.229	0.003	-0.006 to -0.019	0.548
Grey matter fraction	0.440 (±0.010)	0.441 (±0.012)	0.451 (±0.017)	0.451 (±0.011)	-0.002	-0.007 to 0. 003	0.402	-0.005	-0.013 to 0.002	0.142	-0.003	0.010 to 0.005	0.468
Deep grey matter fraction	0.024 (0.001)	0.025 (0.001)	0.026 (0.001)	0.026 (0.001)	**-0.001**	**-0.002 to -0.005**	**0.001**[#]	**-0.002**	**-0.003 to -0.001**	**<0.001**[#]	-0.001	-0.002 to 0.002	0.118
White matter fraction	0.305 (±0.012)	0.311 (±0.012)	0.305 (±0.014)	0.312 (±0.012)	-0.008	-0.015 to -0.002	0.017	-0.003	-0.009 to 0.008	0.925	0.005	-0.003 to 0.014	0.204
Number (%) of patients with cortical lesions	22 (73%)	1/29 (4%)	1/30 (3%)	1/30 (3%)	**0.717**	**0.538 to 0.897**	**<0.001**[#]	**0.694**	**0.488 to 0.900**	**<0.001**[#]	0.038	-0.079 to 0.157	0.515
Number of cortical lesions per participant, median (range)	2 (1 – 14)	1 (0 – 1)	1 (0 – 1)	0	**2.299**	**1.107 to 3.491**	**<0.001**[#]	**2.310**	**0.915 to 3.705**	**0.001**[#]	0.038	-0.079 to 0.157	0.515

Proportion of lesions with CVS/total number of lesions, n (%) (Range)	986/1177 (84%) 25 – 100%	94/285 (33%) 0 – 100% [b]	21/27 (78%) 0 – 100% [c]	0	**44.724**	**34.650 to 54.799**	**<0.001** [#]	14.905	-12.295 to 42.105	0.272	-31.830	-69.194 to 5.533	0.092
Number of white matter lesions with CVS per participant, mean (±SD)	32.9 (±21.7)	3.1 (±4.2)	0.8 (±1.9)	0	**27.447**	**17.819 to 37.075**	**<0.001** [#]	26.545	5.428 to 47.662	0.015	-0.891	-4.840 to 3.057	0.647
Cervical Cord*													
Number (%) of patients with at least one cervical cord lesion	17/31 (55%)	12/30 (40%)	1/28 (4%)	0	0.117	-0.148 to 0.381	0.381	**0.537**	**0.302 to 0.771**	**<0.001** [#]	**0.447**	**0.212 to 0.684**	**0.001** [#]
CSA, mm²	75.50(±10.67)	76.07 (±10.92)	78.52 (±8.70)	84.33 (±7.39)	-1.498	-7.303 to 4.307	0.607	-3.400	-9.799 to 2.979	0.290	-4.306	-11.018 to 2.405	0.204
Cord FA	0.65 (±0.03)	0.62 (±0.07)	0.67 (±0.05)	0.67 (±0.05)	0.022	-0.008 to 0.052	0.141	-0.022	-0.050 to 0.005	0.112	-0.046	-0.088 to -0.004	0.032 [#]
Cord MD, μm²/sec	1.06 (±0.07)	1.11 (±0.13)	1.04 (±0.11)	1.07 (±0.09)	-0.047	-0.105 to 0.012	0.117	0.038	-0.019 to 0.095	0.189	0.094	0.013 to 0.175	0.024 [#]
Cord RD μm²/sec	0.61 (±0.08)	0.67 (±0.16)	0.59 (±0.11)	0.62 (±0.13)	-0.058	-0.126 to 0.099	0.093	0.038	-0.022 to 0.098	0.209	0.102	0.008 to 0.196	0.033 [#]
Cord AD μm²/sec	1.96 (±0.11)	1.98 (±0.11)	1.94 (±0.13)	2.02 (±0.11)	-0.024	-0.082 to 0.034	0.412	0.035	-0.037 to 0.107	0.331	0.075	-0.001 to 0.150	0.053
Optic Nerve^													
***RNFL thickness,* mean (±SD), μm**	87.54 (±13.83)	82.41 (±22.54)	73.54 (±20.33)	100.27 (±10.91)	7.001	-2.609 to 12.610	0.153	**12.911**	**3.288 to 22.594**	**0.009**	5.911	-4.540 to 16.361	0.268
***GCIPL thickness,* mean (±SD), μm**	87.03 (±12.33)	73.14 (±19.68)	75.26 (±16.39)	93.65 (±11.40)	**13.196**	**3.562 to 22.831**	**0.007** [#]	12.220	2.350 to 22.091	0.015	-0.976	-10.528 to 8.575	0.841
***MTR whole optic nerve,* mean (±SD), a.u.**	33.57 (±3.35)	31.40 (±4.06)	30.31 (±3.63)	34.07 (±3.14)	**2.250**	**0.688 to 3.811**	**0.005** [#]	**3.021**	**1.276 to 4.765**	**0.001** [#]	0.771	-1.035 to 2.578	0.403

***MTR intraorbital segment,* mean (±SD), a.u.**	32.37 (±3.56)	28.78 (±5.57)	27.91 (±5.34)	31.67 (±4.17)	**3.777**	**1.688 to 5.865**	**<0.001**[#]	**3.715**	**1.382 to 6.048**	**0.002**[#]	-0.062	-2.477 to 2.352	0.960
***MTR canicular segment,* mean (±SD), a.u.**	34.12 (±4.99)	31.90 (±6.05)	31.73 (±4.85)	35.50 (±4.72)	1.232	-0.887 to 3.351	0.254	2.387	0.014 to 4.759	0.049	1.154	-1.304 to 3.613	0.357
***MTR intracranial segment,* mean (±SD), a.u.**	34.24 (±3.94)	32.50 (±4.23)	31.30 (±4.11)	35.05 (±4.35)	1.768	-0.010 to 3.547	0.051	**2.919**	**0.931 to 4.908**	**0.004**[#]	1.151	-0.909 to 3.211	0.273

Abbreviations: AD=axial diffusivity, a.u.=arbitrary units, CI=confidence interval, CLs=cortical lesions, CSA=cross sectional area, CVS=central vein sign, FA=fractional anisotropy, GCIPL=ganglion cell–inner plexiform layer, MD=mean diffusivity, MTR: magnetization transfer ratio, RC=regression coefficient, RD=radial diffusivity, RNFL: retinal nerve fiber layer SD= standard deviation, SWI=susceptibility weighted imaging.

**Using linear regression models.*

^Using mixed-effects models.

[#] *Significances persist when correcting for sex, age, upgrade of the scanner and disease duration*

[a] *Considering all patients*

[b] *One patient had only one lesion and this lesion showed the CVS (resulting in 100%).*

[c] *One patient had only one lesion and this lesion did not show the CVS (resulting in 0%).*

Table 3: Best discriminators between RRMS and AQP4-NMOSD using logistic regression at patient's level, corrected for age, sex and upgrade of the scanner.

MRI measures	RRMS vs AQP4-NMOSD							
	OR (95% CI)	P-value[#]	Accuracy (%)	Specificity (%)	Sensitivity (%)	AUC	BIC	Best cut-off
Individual measures								
Proportion of lesions with CVS	1.09 (1.05 to 1.14)	<0.001	91	88	93	0.93	49.04	54%
Number of cortical lesions	32.52 (3.52 to 300.03)	0.002	84	90	77	0.91	60.43	1
Number of white matter lesions	1.07 (1.03 to 1.11)	0.001	78	84	73	0.85	69.65	11
Deep grey matter fraction	0.48^ (0.30 to 0.78)	0.003	76	79	73	0.80	82.81	0.022
Brain parenchymal fraction	0.48 (0.28 to 0.83)	0.008	66	72	60	0.76	86.40	0.726
MTR whole optic nerve*	1.32 (1.04 to 1.68)	0.023	66	60	71	0.73	90.58	31.74 a.u.
Combination of measures								

Percentage of lesions with CVS + Number of cortical lesions + MTR whole optic nerve*	1.07 (1.02 to 1.12) 31.01 (1.52 to 634.16) 1.21 (1.02 to 2.03)	<0.001	95	92	97	0.97	44.78	NA

Abbreviations: AUC: area under the curve, BIC: bayesian information criterion, CVS: central vein sign, MTR: magnetization transfer ratio, OR: odd ratio

**For the optic nerve analysis, the average between the two eyes for each patient was used*

#Significances persist when correcting for sex, age, upgrade of the scanner and disease duration

^This OR refers to the analysis for the variable multiplied by 1000

Table 4: Best discriminators between RRMS and MOGAD using logistic regression at patient's level, corrected for age, sex and upgrade of the scanner.

MRI measures	RRMS vs MOGAD							
	OR (95% CI)	P-value[#]	Accuracy (%)	Specificity (%)	Sensitivity (%)	AUC	BIC	Best cut-off
Individual measures								
Number of white matter lesions	1.89 (1.20 to 2.99)	0.006	94	94	93	0.99	26.96	5
Number of cortical lesions	24.68 (2.82 to 215.65)	0.004	84	97	71	0.87	43.15	1
RNFL*	1.06 (1.02 to 1.12)	0.009	80	79	81	0.83	51.06	88 µm
Deep grey matter fraction	0.24^ (0.10 to 0.56)	0.001	79	71	83	0.89	53.75	0.022
Presence of at least one cervical cord lesion	80.01 (4.03 to 1591.84)	0.004	79	56	90	0.86	55.79	1

Combination of measures								
Number of cortical lesions + RNFL*	23.98 (1.36 to 422.75) 1.11 (1.02 to 1.22)	<0.001	84	92	77	0.94	50.52	NA

Abbreviations: AUC: area under the curve, BIC: bayesian information criterion, OR: odd ratio, RNFL: retinal nerve fibre layer

**For the optic nerve analysis, the average between the two eyes for each patient was used*

[#]Significances persist when correcting for sex, age, upgrade of the scanner and disease duration

^This OR refers to the analysis for the variable multiplied by 1000

WNL-2022-201326_sup --- http://links.lww.com/WNL/C402

References

1. Thompson AJ, Banwell BL, Barkhof F, et al. Diagnosis of multiple sclerosis: 2017 revisions of the McDonald criteria. *Lancet Neurol*. 2018;17(2):162-173. doi:10.1016/S1474-4422(17)30470-2
2. Waters P, Woodhall M, O KC, et al. MOG cell-based assay detects non-MS patients with inflammatory neurologic disease. *Neurol Neuroimmunol Neuroinflamm*. 2015;2:89. doi:10.1212/NXI.0000000000000089
3. Waters PJ, Komorowski L, Woodhall M, et al. A multicenter comparison of MOG-IgG cell-based assays. Published online 2019. doi:10.1212/WNL.0000000000007096
4. Waters PJ, McKeon A, Leite MI, et al. Serologic diagnosis of NMO: A multicenter comparison of aquaporin-4-IgG assays. *Neurology*. 2012;78(9):665-671. doi:10.1212/WNL.0b013e318248dec1
5. Marchionatti A, Woodhall M, Waters PJ, Sato DK. Detection of MOG-IgG by cell-based assay: moving from discovery to clinical practice. *Neurol Sci*. 2021;42(1):73-80. doi:10.1007/s10072-020-04828-1
6. Sechi E, Buciuc M, Pittock SJ, et al. Positive Predictive Value of Myelin Oligodendrocyte Glycoprotein Autoantibody Testing. *JAMA Neurol*. 2021;78(6):741-746. doi:10.1001/jamaneurol.2021.0912
7. Waters P, Fadda G, Woodhall M, et al. Serial Anti-Myelin Oligodendrocyte

Glycoprotein Antibody Analyses and Outcomes in Children with Demyelinating Syndromes. *JAMA Neurol*. 2020;77(1):82-93. doi:10.1001/jamaneurol.2019.2940

8. Pisani F, Sparaneo A, Tortorella C, et al. Aquaporin-4 autoantibodies in neuromyelitis optica: AQP4 isoform-dependent sensitivity and specificity. *PLoS One*. 2013;8(11). doi:10.1371/journal.pone.0079185
9. Matsuoka T, Matsushita T, Kawano Y, et al. Heterogeneity of aquaporin-4 autoimmunity and spinal cord lesions in multiple sclerosis in Japanese. *Brain*. 2007;130(5):1206-1223. doi:10.1093/brain/awm027
10. Matthews L, Marasco R, Jenkinson M, et al. Distinction of seropositive NMO spectrum disorder and MS brain lesion distribution. *Neurology*. 2013;80(14):1330-1337. doi:10.1212/WNL.0b013e3182887957
11. Duan Y, Zhuo Z, Li H, et al. Brain structural alterations in MOG antibody diseases: A comparative study with AQP4 seropositive NMOSD and MS. *J Neurol Neurosurg Psychiatry*. Published online 2021. doi:10.1136/jnnp-2020-324826
12. Filippi M, Preziosa P, Banwell BL, et al. Assessment of lesions on magnetic resonance imaging in multiple sclerosis: practical guidelines. *Brain*. 2019;142(7):1858-1875. doi:10.1093/brain/awz144
13. Kim HJ, Paul F, Lana-Peixoto MA, et al. MRI characteristics of neuromyelitis optica spectrum disorder: an international update. *Neurology*. 2015;84(11):1165-1173. doi:10.1212/WNL.0000000000001367
14. Cobo-Calvo A, Ruiz A, Maillart E, et al. Clinical spectrum and prognostic value of CNS MOG autoimmunity in adults: The MOGADOR study. *Neurology*. 2018;90(21):e1858-e1869. doi:10.1212/WNL.0000000000005560
15. Ciccarelli O, Cohen JA, Reingold SC, et al. Spinal cord involvement in multiple sclerosis and neuromyelitis optica spectrum disorders. *Lancet Neurol*. 2019;18(2):185-

197. doi:10.1016/S1474-4422(18)30460-5

16. Sechi E, Krecke KN, Messina SA, et al. Comparison of MRI Lesion Evolution in Different Central Nervous System Demyelinating Disorders. *Neurology*. 2021;97(11):e1097-e1109. doi:10.1212/WNL.0000000000012467

17. Geraldes R, Ciccarelli O, Barkhof F, et al. The current role of MRI in differentiating multiple sclerosis from its imaging mimics. *Nat Rev Neurol*. 2018;14(4):199-213. doi:10.1038/nrneurol.2018.14

18. Thompson AJ, Banwell BL, Barkhof F, et al. Diagnosis of multiple sclerosis: 2017 revisions of the McDonald criteria. *Lancet Neurol*. 2018;17(2):162-173. doi:10.1016/S1474-4422(17)30470-2

19. Calabrese M, Oh MS, Favaretto A, et al. No MRI evidence of cortical lesions in neuromyelitis optica. *Neurology*. 2012;79(16):1671-1676. doi:10.1212/WNL.0b013e31826e9a96

20. Messina S, Mariano R, Roca-Fernandez A, et al. Contrasting the brain imaging features of MOG-antibody disease, with AQP4-antibody NMOSD and multiple sclerosis: *https://doi.org/101177/13524585211018987*. Published online May 28, 2021. doi:10.1177/13524585211018987

21. Cortese R, Magnollay L, Tur C, et al. Value of the central vein sign at 3T to differentiate MS from seropositive NMOSD Criteria for rating therapeutic and diagnostic studies. 2018;90:1183-1190. doi:10.1212/WNL.0000000000005256

22. Ciotti JR, Eby NS, Brier MR, et al. Central vein sign and other radiographic features distinguishing myelin oligodendrocyte glycoprotein antibody disease from multiple sclerosis and aquaporin-4 antibody-positive neuromyelitis optica. *Mult Scler J*. Published online April 19, 2021:135245852110070. doi:10.1177/13524585211007086

23. Matthews L, Kolind S, Brazier A, et al. Imaging Surrogates of Disease Activity in

Neuromyelitis Optica Allow Distinction from Multiple Sclerosis. Bradl M, ed. *PLoS One*. 2015;10(9):e0137715. doi:10.1371/journal.pone.0137715

24. Chien C, Scheel M, Schmitz-Hübsch T, et al. Spinal cord lesions and atrophy in NMOSD with AQP4-IgG and MOG-IgG associated autoimmunity. *Mult Scler J*. Published online 2018:1926-1936. doi:10.1177/1352458518815596

25. Mariano R, Messina S, Roca-Fernandez A, Leite MI, Kong Y, Palace JA. Quantitative spinal cord MRI in MOG-antibody disease, neuromyelitis optica and multiple sclerosis. *Brain*. Published online 2020:1-15. doi:10.1093/brain/awaa347

26. Flanagan EP. Neuromyelitis optica spectrum disorder and other non-multiple sclerosis central nervous system inflammatory diseases. *Contin Lifelong Learn Neurol*. 2019;25(3):815-844. doi:10.1212/CON.0000000000000742

27. Silbermann E, Wooliscroft L, Bourdette D. Using the Anterior Visual System to Assess Neuroprotection and Remyelination in Multiple Sclerosis Trials. *Curr Neurol Neurosci Rep*. 2017;18(8):1-9. doi:10.1007/s11910-018-0858-y

28. Trip SA, Schlottmann PG, Jones SJ, et al. Optic nerve magnetization transfer imaging and measures of axonal loss and demyelination in optic neuritis. *Mult Scler*. 2007;13(7):875-879. doi:10.1177/1352458507076952

29. Klistorner A, Chaganti J, Garrick R, Moffat K, Yiannikas C. Magnetisation transfer ratio in optic neuritis is associated with axonal loss, but not with demyelination. *Neuroimage*. 2011;56(1):21-26. doi:10.1016/j.neuroimage.2011.02.041

30. Filippatou AG, Mukharesh L, Saidha S, Calabresi PA, Sotirchos ES. AQP4-IgG and MOG-IgG Related Optic Neuritis—Prevalence, Optical Coherence Tomography Findings, and Visual Outcomes: A Systematic Review and Meta-Analysis. *Front Neurol*. 2020;11:540156. doi:10.3389/fneur.2020.540156

31. Outteryck O, Majed BILAL, Defoort-Dhellemmes S, Vermersch P, Zéphir H. A

comparative optical coherence tomography study in neuromyelitis optica spectrum disorder and multiple sclerosis. *Mult Scler*. 2015;21(14):1781-1793. doi:10.1177/1352458515578888

32. Stiebel-Kalish H, Lotan I, Brody J, et al. Retinal Nerve Fiber Layer May Be Better Preserved in MOG-IgG versus AQP4-IgG Optic Neuritis: A Cohort Study. Paul F, ed. *PLoS One*. 2017;12(1):e0170847. doi:10.1371/journal.pone.0170847
33. Wingerchuk DM, Banwell B, Bennett JL, et al. International consensus diagnostic criteria for neuromyelitis optica spectrum disorders. *Neurology*. 2015;85(2):177-189. doi:10.1212/WNL.0000000000001729
34. Marignier R, Hacohen Y, Cobo-Calvo A, et al. Myelin-oligodendrocyte glycoprotein antibody-associated disease. *Lancet Neurol*. 2021;20(9):762-772. doi:10.1016/S1474-4422(21)00218-0
35. Fischer JS, Rudick RA, Cutter GR, Reingold SC. The multiple sclerosis functional composite measure (MSFC): An integrated approach to MS clinical outcome assessment. In: *Multiple Sclerosis*. Vol 5. ; 1999:244-250. doi:10.1177/135245859900500409
36. Tewarie P, Balk L, Costello F, et al. The OSCAR-IB Consensus Criteria for Retinal OCT Quality Assessment. Villoslada P, ed. *PLoS One*. 2012;7(4):e34823. doi:10.1371/journal.pone.0034823
37. Cardoso MJ, Modat M, Wolz R, et al. Geodesic Information Flows: Spatially-Variant Graphs and Their Application to Segmentation and Fusion. *IEEE Trans Med Imaging*. 2015;34(9):1976-1988. doi:10.1109/TMI.2015.2418298
38. Prados F, Cardoso MJ, Kanber B, et al. A multi-time-point modality-agnostic patch-based method for lesion filling in multiple sclerosis. *Neuroimage*. 2016;139:376-384. doi:10.1016/j.neuroimage.2016.06.053

39. Sethi V, Yousry TA, Muhlert N, et al. Improved detection of cortical MS lesions with phase-sensitive inversion recovery MRI. *J Neurol Neurosurg Psychiatry*. 2012;83(9):877-882. doi:10.1136/jnnp-2012-303023

40. Sati P, Oh J, Todd Constable R, et al. The central vein sign and its clinical evaluation for the diagnosis of multiple sclerosis: a consensus statement from the North American Imaging in Multiple Sclerosis Cooperative. *Nat Publ Gr*. Published online 2016. doi:10.1038/nrneurol.2016.166

41. Horsfield MA, Sala S, Neema M, et al. Rapid semi-automatic segmentation of the spinal cord from magnetic resonance images: application in multiple sclerosis. *Neuroimage*. 2010;50(2):446-455. doi:10.1016/j.neuroimage.2009.12.121

42. M J, CF B, TE B, MW W, SM S. FSL. *Neuroimage*. 2012;62(2):782-790. doi:10.1016/J.NEUROIMAGE.2011.09.015

43. De Leener B, Lévy S, Dupont SM, et al. SCT: Spinal Cord Toolbox, an open-source software for processing spinal cord MRI data. *Neuroimage*. 2017;145:24-43. doi:10.1016/J.NEUROIMAGE.2016.10.009

44. Höftberger R, Guo Y, Flanagan EP, et al. The pathology of central nervous system inflammatory demyelinating disease accompanying myelin oligodendrocyte glycoprotein autoantibody. *Acta Neuropathol*. 2020;(0123456789). doi:10.1007/s00401-020-02132-y

45. Sharma R, Fischer MT, Bauer J, et al. Inflammation induced by innate immunity in the central nervous system leads to primary astrocyte dysfunction followed by demyelination. *Acta Neuropathol*. 2010;120(2):223-236. doi:10.1007/s00401-010-0704-z

46. Uzawa A, Mori M, Kuwabara S. Different patterns of brainstem and cerebellar MRI abnormalities in demyelinating disorders with MOG and aquaporin-4 antibodies. *J*

Neurol Neurosurg Psychiatry. 2021;92(4):348. doi:10.1136/jnnp-2020-325503

47. Bouman PM, Steenwijk MD, Pouwels PJW, et al. OUP accepted manuscript. *Brain*. Published online 2020. doi:10.1093/brain/awaa233

48. Narayan RN, McCreary M, Conger D, Wang C, Greenberg BM. Unique characteristics of optical coherence tomography (OCT) results and visual acuity testing in myelin oligodendrocyte glycoprotein (MOG) antibody positive pediatric patients. *Mult Scler Relat Disord*. 2019;28:86-90. doi:10.1016/j.msard.2018.11.026

49. Eshaghi A, Wottschel V, Cortese R, et al. Gray matter MRI differentiates neuromyelitis optica from multiple sclerosis using random forest. *Neurology*. 2016;87(23). doi:10.1212/WNL.0000000000003395

50. Sastre-Garriga J, Pareto D, Battaglini M, et al. MAGNIMS consensus recommendations on the use of brain and spinal cord atrophy measures in clinical practice. *Nat Rev Neurol*. 2020;16(3):171-182. doi:10.1038/s41582-020-0314-x

Figure Legends

Figure 1: Differences in brain and cervical cord measures between RRMS, AQP4-NMOSD, MOGAD and healthy controls.

The boxplots show lower number and volume of lesions and higher degree of atrophy in RRMS than AQP4-NMOSD and MOGAD patients and healthy controls.

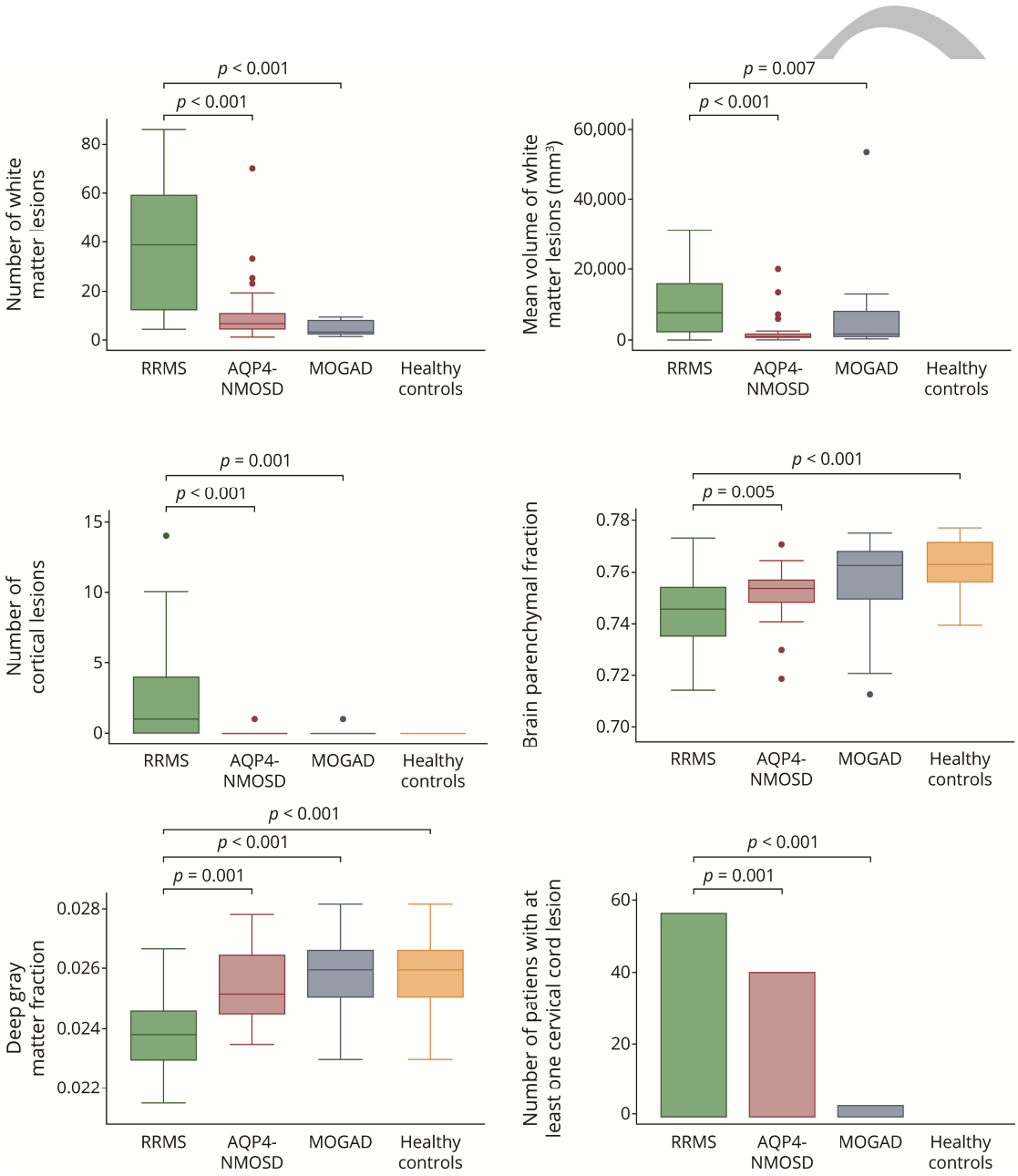

Figure 2: Examples of cortical lesions seen on phase sensitive inversion recovery images (PSIR) and lesions with and without the central vein sign (CVS) on susceptibility-weighted imaging (SWI) in RRMS, AQP4-NMOSD, MOGAD.

In the upper figures, PSIR imaging showing lesions located exclusively in the cortex (intracortical, red arrow) or within the cortex and adjacent juxtacortical white matter (leukocortical, blue arrow) in RRMS, AQP4-NMOSD and MOGAD. Intracortical and leukocortical lesions were detected in RRMS patients (a), while one leukocortical lesion in one AQP4-NMOSD patient (b) and one intracortical in one MOGAD patient (c) were found.

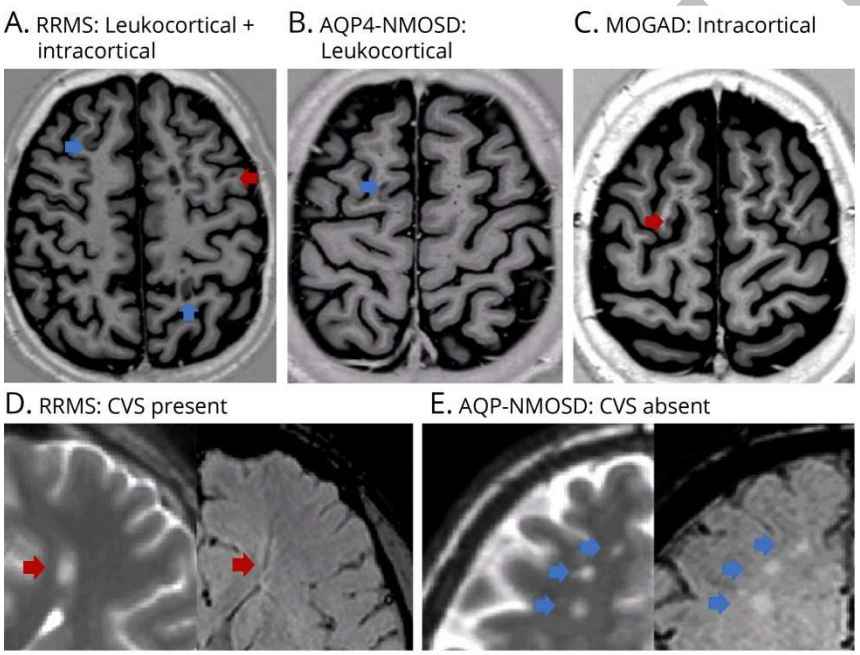

Figure 3: Central vein sign (CVS) detected on susceptibility-weighted imaging (SWI) in the patient groups.

The scatterplot shows the proportion of lesions with CVS (out of the total number of lesions) for each patient in the three diseases (orange=RRMS, green=AQP4-NMOSD, blue=MOGAD). Patients without brain lesions are not displayed. 2/8 MOGAD patients were excluded from the rating (one for bad SWI quality, one for extensive, confluent PD/T2 abnormalities).

Footnote: 100% means that all lesions assessed showed the CVS

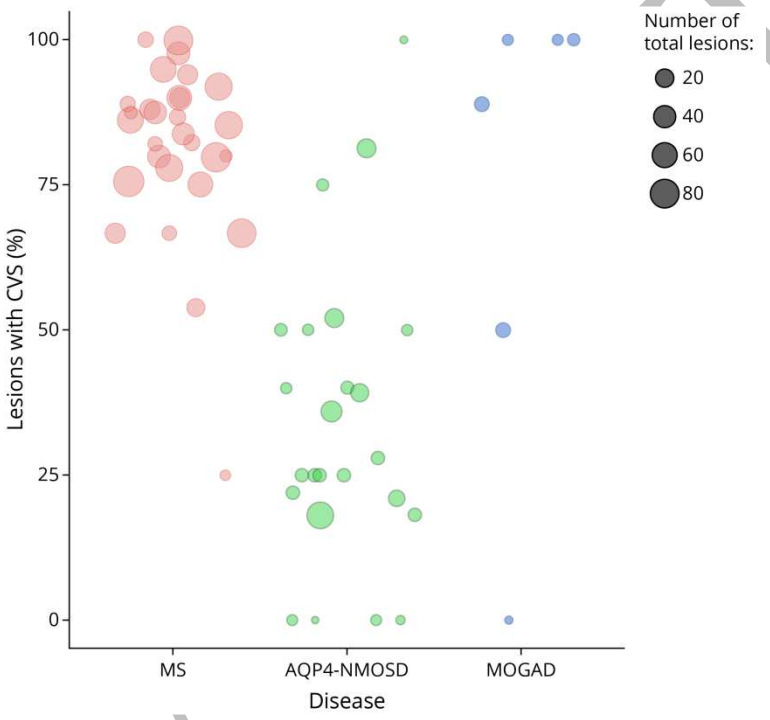

Differentiating Multiple Sclerosis From AQP4-Neuromyelitis Optica Spectrum Disorder and MOG-Antibody Disease With Imaging

Rosa Cortese, Ferran Prados Carrasco, Carmen Tur, et al.

Neurology published online October 3, 2022
DOI 10.1212/WNL.0000000000201465